Development of a 2D finite element model for the investigation of the tread braked railway wheels thermo-mechanical behaviour

Development of a 2D finite element model for the investigation of the tread braked railway wheels thermo-mechanical behaviour

To cite this article: M Magelli 2022 *IOP Conf. Ser.: Mater. Sci. Eng.* **1214** 012041

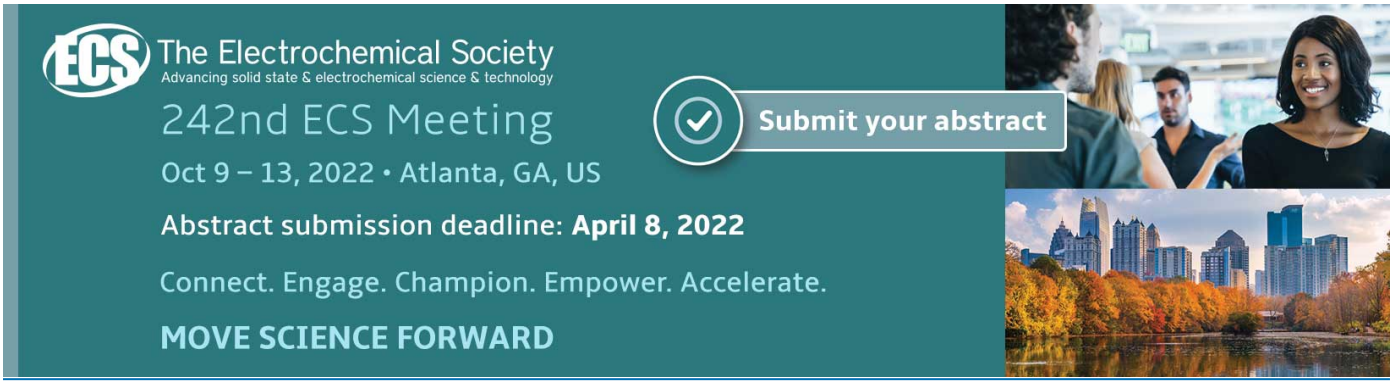

Development of a 2D finite element model for the investigation of the tread braked railway wheels thermo-mechanical behaviour

M Magelli

Politecnico di Torino, Department of Mechanical and Aerospace Engineering, C.so Duca degli Abruzzi 24, 10129, Torino

matteo.magelli@polito.it

Abstract. The main drawback of tread braking is the rail wheel heating due to friction sliding. Thermal stresses and strains can lead to wheel surface damages while at the same time fast cooling from high temperature can cause microstructural changes, with possible local formation of brittle martensite. Nowadays, the investigation of the wheel and shoe thermomechanical interaction is typically performed using finite element (FE) codes. The paper shows the development, implementation and preliminary validation of a 2D plane FE model for the calculation of the thermal field produced in a tread braked wheel due to drag and stop braking operations. The model includes a structural contact module for the static calculation of the normal and tangential contact pressure at the wheel-shoe interface and a thermal transient module, which computes the wheel temperature considering the friction heat flux and the cooling due to air convection and rail chill.

1. Introduction

Tread braking is the braking system traditionally installed on freight wagons, however other applications in the railway field include metro vehicles and locomotives, where tread braking acts as a support to electrodynamic braking or as a back-up in case of failure of the dynamic braking system. The working principle of tread braking is based on the friction forces generated at the wheel-shoe interface when a brake block is pressed against the wheel surface. With respect to disc braking, tread braking features several benefits, mainly low costs, ease of installation, reduction of the wheelset mass and rotational inertia and the generation of a polishing effect on the wheel surface, which can improve the wheel-rail contact conditions [1]. Nevertheless, the generation of friction forces at the wheel-shoe interface necessarily leads to friction heating of the wheel itself, possibly causing local damages on the wheel surface or even local changes in the wheel steel microstructure, with formation of brittle martensite, in case a quick cooling occurs from high temperature. The friction heat partitioning between the wheel and the brake shoe is strongly dependent on the brake shoe configuration and material, as nowadays P10 (cast iron with phosphorus) shoes are being replaced by composite ones. These new compounds are specifically designed with the aim to reduce rolling noise [2,3], however, due to their composition, a higher percentage of the total friction heat flows into the wheel rather than into the shoe [4]. Moreover, composite shoes can feature a wide range of frictional characteristics according to their composition [5,6].

Due to the reason mentioned above, it is essential to gain a good understanding of the wheel thermal behavior consequent to tread braking, in order to optimize braking operations, to design new brake shoe compounds and to enhance the safety of the whole vehicle. Furthermore, the availability of a wheel-shoe thermal model is an essential tool for the development of new air brake monitoring systems [7-9]. Since it is not an easy task to perform on track tests to study the wheel-shoe thermomechanical behavior, due to issues

related to high costs, interruption of the line traffic, long times, poor reproducibility of test conditions, and impossibility to analyze all the operating conditions of interest, numerical simulations seem to be the most promising strategy for the investigation of this phenomenon. Although the railway literature witnesses analytical model for the calculation of the temperature field due to friction heating at the wheel-rail and wheel-shoe contact interfaces [10-13], the most common approach nowadays is finite element (FE) codes, implemented in commercial software packages, thanks to the huge computational power of modern computers. The models developed for the investigation of the temperature field arising in tread braked wheels are typically either 3D [14-17] or 2D axisymmetric [3,4,18,19], but 3D models, despite being able to be the most accurate solution, are computationally demanding, while the main drawback of 2D axisymmetric models is that they only consider average values of the heat flows in circumferential direction, thus only computing an average value of the wheel tread. Therefore, they struggle in the computation of local hot spots which are the main source of microstructural changes and local defects. Finally, also 2D plane models [20-23] exist, which however commonly perform an a priori assumption of the wheel-shoe contact pressure distribution.

The present work shows the development of a 2D plane FE model, implemented in the commercial software package ANSYS Mechanical APDL, able to compute the temperature field of a tread braked wheel. The model includes a static structural contact module, which computes the contact pressure distribution, and a transient thermal module, which calculates the wheel thermal field due to tread braking, taking into account the friction heat, the air convection and the rail chill effect. The FE model can reproduce both 1Bg and 2Bg block configurations in drag and stop braking operations, but the present paper only deals with drag braking, which is considered to be more harmful for the wheel from a thermal point of view. The main inputs for the FE models are calculated by means of an external Matlab routine. To save the total computational time, the mechanical and thermal problems are decoupled, i.e., the contact module runs first to compute the pressure distribution, and then the outputs of this module are used to compute the friction heat flowing into the wheel, which becomes the main input of the thermal module performing the calculation of the wheel thermal field.

The paper is organized as follows: the next section describes the model structure and the modelling strategy, then focus is given to the implementation of the contact and thermal modules in ANSYS Mechanical APDL. Finally, the main outputs obtained from the preliminary simulations performed with the codes are shown, and conclusions are drawn also giving emphasis to the future upgrades needed by the code and to the future developments of the activity.

2. Model description

The tool described in the present paper includes three main modules, i.e., an external Matlab routine, a FE static contact module and a FE transient thermal module. The Matlab routine computes the main parameters related to the braking operation based on the longitudinal vehicle dynamics according to the prescription of the UIC 544-1 leaflet [24], and it was built starting from an existing longitudinal train dynamic simulator developed by the author's research group [25,26]. The static contact module calculates the normal and tangential pressure distributions which are then used in the transient thermal module to compute the evolution of the wheel temperature during the drag or stop braking operation, using a decoupled approach. Figure 1 sketches the structure of the tool described thoroughly in the present paper.

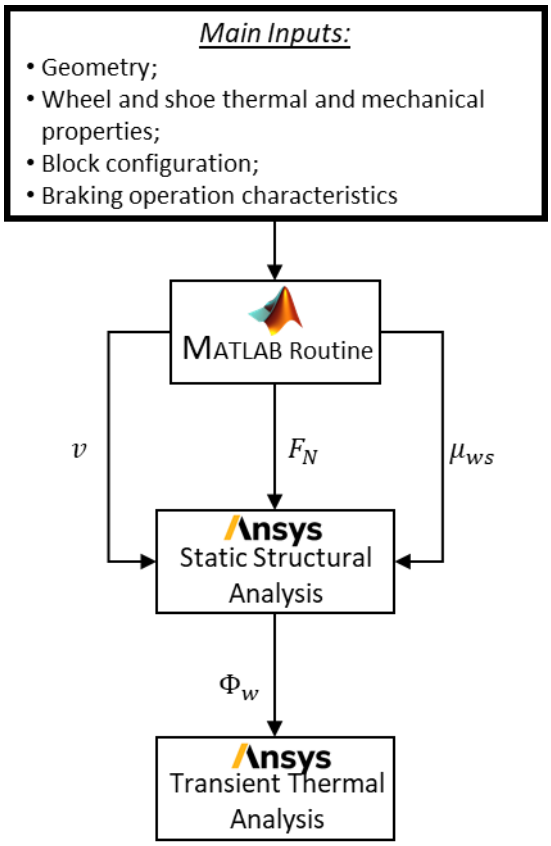

Figure 1. Scheme of the proposed tool for the simulation of the thermo-mechanical behaviour of tread braked wheels.

The Matlab routine relies on the equations of the vehicle longitudinal equilibrium and of the wheelset rotational equilibrium, written under the simplifying hypothesis that the braking effort is distributed uniformly among all wheelsets of the vehicle, see equations 1 and 2. Please note that in equations 1 and 2, M_w is the wagon weight (kg), g is gravity acceleration, i_s is the track slope (‰), $\ddot{x}$ is the vehicle deceleration, N_{ax} is the number of wheelsets of the vehicle, F_x is the longitudinal wheel-rail force acting on the wheelset, C_B is the braking torque on the wheelset, J_{yy} is the wheelset rotational inertia, $\dot{\omega}$ is the wheelset deceleration, r is the wheel radius and finally F_{Res} is the sum of the rolling and aerodynamic resistant forces. Although the last term can be calculated according to different expressions as a function of the vehicle speed $\dot{x}$ [27], the modified Davis's equation, suggested in the international benchmark of longitudinal dynamics simulators [28,29] is used, see equation 3, as it features an explicit dependency on the vehicle mass. The braking torque acting on the wheelset is related to the pressing force acting at the wheel-shoe interface F_b according to equation 4, in which N_{ws} is the number of blocks per wheel and μ_{ws} is the wheel-shoe friction coefficient. For cast iron brake shoes, the latter can be calculated as a function of the wheel-shoe pressing force F_N, and the relative speed V_s, using the Karwatzki's equation, see equation 5, in which the normal force and the relative speed must be expressed in kN and km/h, respectively. The inputs for the simulation of a drag braking operation are the vehicle running speed and the track slope. Moreover, since the vehicle is running at constant speed, the wagon and wheelset decelerations are equal to zero. Therefore, it is easy to calculate the wheel-rail longitudinal contact force from equation 1 and then the braking torque from equation 2. Then, the wheel-shoe normal contact force is obtained by solving equations 4 and 5 using the Newton-Raphson's method [30]. The Matlab routine was validated against the UIC-approved TrainDy software package [31], with a good agreement between the outputs computed by the two codes in the same simulation scenarios.

$$\frac{M_w g i_s}{1000} + M_w \ddot{x} - F_{Res} - N_{ax} F_x = 0 \quad (1)$$

$$C_B = J_{yy}\dot{\omega} + F_x r \tag{2}$$

$$F_{Res} = \frac{M_w}{1000}\left(2.943 + 89200\frac{N_{ax}}{M_w} + 0.11\dot{x} + \frac{1581\dot{x}^2}{M_w}\right) \tag{3}$$

$$C_B = 2N_{ws}\mu_{ws}F_N r \tag{4}$$

$$\mu_{wb} = 0.6\frac{V_s + 100}{5V_s + 100}\frac{16/g\,F_N + 100}{80/g\,F_N + 100} \tag{5}$$

Shifting focus to the contact module, it performs the calculation of the normal and tangential contact pressures at the wheel-shoe contact interface starting from the knowledge of the pressing force and of the wheel-shoe friction coefficient and it can deal with both 1Bg and 2Bg block configurations. The wheel-shoe contact is solved using the finite element methods, applying the augmented Lagrangian algorithm [32], with an automatic update of the normal contact stiffness at each iteration. The contact algorithm considers the effects of sliding and friction at the wheel-shoe contact interface, and a constant friction coefficient is defined, since the wheel-shoe contact is a sliding contact and therefore the transition between static and dynamic friction coefficient does not occur.

Finally, once the contact problem is solved, the normal and tangential pressure distributions are used to calculate the total friction heat generated at the wheel-shoe contact interface Φ_{tot}, while the portion of heat flowing into the wheel Φ_w, which is the main input of the thermal module, is calculated introducing a partitioning factor α, see equations 6-9, in which θ is the angular coordinate, V_s is the sliding speed, κ is the thermal diffusivity, λ is the thermal conductivity, ρ is density, c is specific heat, S is the contact area and finally b and w refer to the block and wheel, respectively. The thermal module considers the dependency of the wheel thermal properties on speed using polynomial regression from experimental data available in the literature [33], however for the sake of ease of implementation, the partitioning factor is computed only once at the beginning of the simulation, using the values calculated at 100°C.

$$\Phi_{tot}(\vartheta) = \mu_{ws}p_n(\vartheta)V_s \tag{6}$$

$$\Phi_w(\vartheta) = \alpha\Phi_{tot}(\vartheta) \tag{7}$$

$$\alpha = \left\{1 + \left(\frac{\kappa_w}{\kappa_b}\right)^{\frac{1}{2}}\frac{\lambda_b}{\lambda_w}\frac{S_b}{S_w}\right\}^{-1} \tag{8}$$

$$\kappa_{w/b} = \frac{\lambda_{w/b}}{\rho_{w/b}c_{w/b}} \tag{9}$$

The thermal module also considers the wheel cooling due to convection with ambient air and rail chill effect, as schematically shown in figure 2 for a tread braked wheel with 1Bg block configuration. The air convection coefficient depends on the wheel translational speed, and it is calculated according to the Churchill and Bernstein's correlation [34], see equations 10-13, where Nu is the Nusselt Number, Re is the Reynolds number, Pr is the Prandtl number, V_x is the wheel translational speed, r is the wheel radius, λ, ν and c are thermal conductivity, kinematic viscosity and mass specific heat, respectively, and finally subscript a refers to air properties.

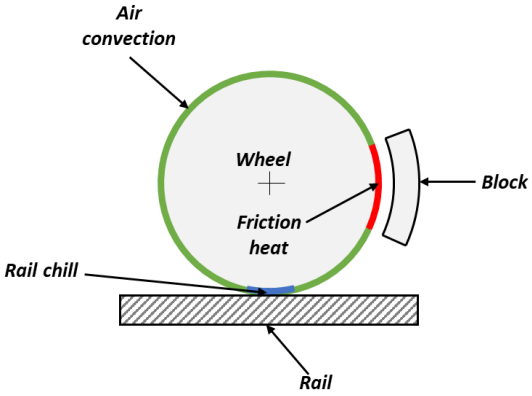

Figure 2. Sketch of the heat fluxes acting on a tread braked wheel (example for 1Bg configuration).

$$h_a = \frac{Nu\lambda_a}{2r} \tag{10}$$

$$Nu = 0.3 + \frac{0.62(Re)^{1/2}(Pr)^{1/3}}{\left[1+\left(\frac{0.4}{Pr}\right)^{2/3}\right]^{1/4}}\left[1+\left(\frac{Re}{282000}\right)^{5/8}\right]^{4/5} \tag{11}$$

$$Re = \frac{2rV_x}{\nu_a} \tag{12}$$

$$Pr = \frac{\rho_a \nu_a c_a}{\lambda_a} \tag{13}$$

Lastly, the rail chill effect, which is physically a conductive phenomenon, is treated by introducing an equivalent convection coefficient h_{rc}, only applied to the portion of the wheel which is in contact with the cooler rail, following the approach stated by Vakkalagadda et al. [4]. The convection coefficient h_{rc} is calculated as a function of the wheel translational speed V_x, assuming that the slip at the contact interface is negligible, of the longitudinal semi-axis of the contact ellipse a_x, calculated according to the Hertzian theory, and of the wheel and rail thermal effusivity β, see equations 14-17, in which σ_{wr} represents the wheel-rail thermal conductance and subscripts r and w refer to the rail and wheel, respectively.

$$\sigma_{wr} = \frac{14\gamma\beta_r(V_x)^{1/2}}{(2\pi)^{3/2}(a_x)^{1/2}} \tag{14}$$

$$\gamma = \left(1+\frac{\beta_r}{\beta_w}\right)^{-1} \tag{15}$$

$$\beta_{w/r} = \left(\lambda_{w/r}\rho_{w/r}c_{w/r}\right)^{1/2} \tag{16}$$

$$h_{rc} = \frac{a_x\sigma_{wr}}{4r} \tag{17}$$

3. Implementation of the FE modules

Both the contact and thermal FE models are implemented in the commercial software package ANSYS Mechanical APDL. The contact module is a 2D static structural model of the wheel-shoe contact, which can be used for both the 1Bg and 2Bg configurations. Figure 3 shows the wheel-shoe contact model built for a 2Bg block configuration. The wheel is represented as a hollow disc, with an external radius equal to 460 mm and an inner radius equal to 80 mm, thus not reproducing for the sake of simplicity the real wheel profile in axial direction. On the other hand, each block is represented as a circular sector with a length of 320 mm and a radial

thickness equal to 60 mm, in accordance with the standard dimensions for Bg blocks [35]. Both the wheel and the block are meshed with the bidimensional, 8-node quadratic PLANE183 elements, featuring two degrees of freedom (d.o.fs) per node, assuming plane stress conditions and setting the axial width of both elements to 80 mm. The d.o.f of the wheel nodes lying at the inner radius in circumferential direction is suppressed, in order to avoid the wheel rotation, however the contact module accounts for the wheel spinning by means of the CMROTATE command. The brake block holder is not modelled in detail, so it is simply represented by means of a set of MPC184 elements, which are defined such that they behave as rigid links, transferring the load uniformly to the brake block, under the hypothesis that the brake block is far less stiff than its holder. Each rigid beam of the same block is connected to an external node, placed 607 mm away from the wheel center in radial direction, on which the pressing force calculated by means of the external Matlab routine is imposed. The external nodes are constrained so that their translation along the y-axis is prevented, while they are free to move along the x direction. The wheel-shoe conformal contact is faced introducing bi-dimensional surface-to surface contact elements, namely a layer of 3-node CONTA172 elements placed on the wheel outer periphery paired with a corresponding layer of TARGE169 elements, placed on the brake shoe inner surface. The conformal wheel-shoe contact problem is solved using the augmented Lagrangian method, adjusting the normal contact stiffness automatically at each iteration, depending on the mean stress of the underlying PLANE183 elements, so that a satisfying trade-off between computational time and good conditioning of the contact matrix can be reached. Since the contact problem is nonlinear, the solution is obtained by means of the Newton-Raphson iteration scheme, forcing the solver not to perform a stiffness matrix symmetrization to improve convergence.

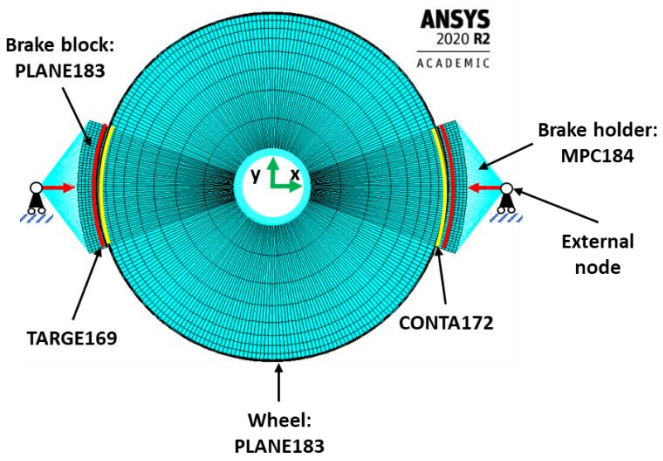

Figure 3. Wheel and block mesh in the contact module for 2Bg block configuration.

On the other hand, the thermal module is a 2D FE transient module which is able to compute the evolution of the wheel temperature during braking operations. In order to reduce the number of d.o.fs of the model and to consequently improve the computing speed, only a 45° circular sector of the wheel is modelled, see figure 4, under the assumption that the heat flux conduction inside the wheel in circumferential direction is negligible with respect to the conduction in radial direction. Simulations not presented in the paper were performed under the same scenarios with the reduced model and a model of the entire wheel, and a good agreement between the outputs of the two models was observed, thus confirming the validity of the hypothesis. The wheel is meshed by means of the 8-node quadratic PLANE77 elements, with a single d.o.f corresponding to the node temperature, setting the element behavior to plane with specification of axial thickness. The thermal boundary conditions are applied to overlying layers of 2-node SURF151 elements, specifying a plane behavior with thickness definition. As noticeable from figure 4, five sets of SURF151 elements are introduced in the model. The lateral edges and the inner radius of the wheel are covered with elements to which an adiabatic condition is superimposed, while the nodes at the outer radius are overlaid with two layers of SURF151 elements, one for the application of the friction heat flux and one for convection boundary condition, with the latter including

both the convection with ambient air and the rail chill effect, which is treated as a convective phenomenon despite being a conductive heat transfer, as previously mentioned.

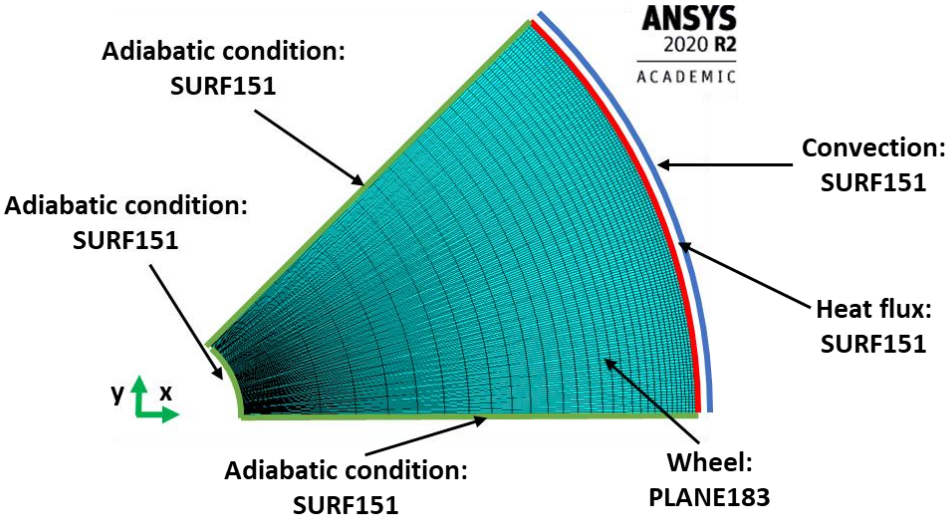

Figure 4. Mesh of the thermal module.

The application of the thermal loads accounts for the wheel rotation, however in the model the wheel is fixed and the thermal loads are rotated thanks to the definition of tables, which are a specific ANSYS built-in data type used for the definition of time and space varying loads. Tables in the models act as 3D look-up tables defining the value of the thermal load at specific time steps and angular coordinates, so that values at intermediate points are automatically calculated through simple interpolations. The thermal problem is described in ANSYS by a system of nonlinear ordinary differential equations (o.d.es), and it is solved using the Crank-Nicolson [36] scheme for numerical integration, enabling the predictive-corrector ANSYS built-in algorithm for automatic adjustment of the time step-size at each iteration and the Newton-Raphson algorithm for the solution of the nonlinear algebraic system obtained at each time step.

4. Preliminary results

This section presents the outputs obtained by the preliminary simulations performed with the contact and thermal modules. Due to the lack of experimental data, it is not easy an easy task to validate the code, however these preliminary simulations were run to assess that the outputs produced by the code are in line with the expectations. The preliminary simulations were run considering the properties of P10 brake shoes, however the code can be launched considering different shoe compounds.

Figure 5 shows the distribution of the wheel-shoe normal contact pressure computed both neglecting and considering the effect of friction and sliding at the contact interface. Two values of the normal force are considered in the plot, i.e., 28.3 and 40 kN, respectively. The former is the pressing force exerted on a reference four-axled freight wagon when the braking pressure is equal to 3.8 bar, while the latter corresponds to the maximum value considered by the UIC 544-1 leaflet for the Bg block configuration. As expected, the maximum value of the contact pressure increases if the normal force is larger. Furthermore, when friction and sliding are taken into account, the pressure distribution is asymmetric, and a peak at the leading edge is noticeable, due to a block jamming effect. The asymmetry of pressure distribution is not surprising, as the resulting contact force must always pass through the external node, to ensure the rotational equilibrium of the block.

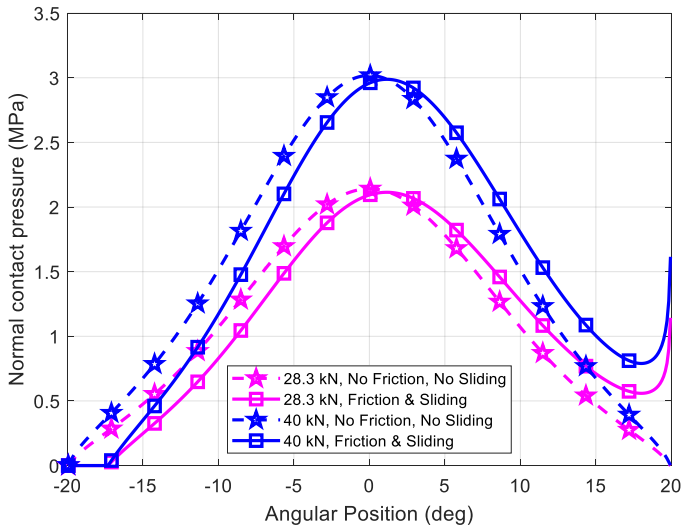

Figure 5. Effect of frictional sliding and normal force on the normal contact pressure distribution computed by the contact module.

A second simulation was run to identify the differences in the wheel temperature with 1Bg and 2Bg block configurations for the same drag braking operation on a 20-ton axle-load freight vehicle, considering the operational parameters suggested by the EN 13979 standard [37], i.e., track slope equal to 21‰ and running speed of 60 km/h. To reduce the computational times, a short-lasting manoeuvre is considered, and the simulation time is equal to 2 minutes, corresponding to a total braking distance of approximately 2 km. Obviously, in case the braking effort is exerted with a single block, the normal force is higher, and the Matlab routine computes a normal force of 13.84 kN and a friction coefficient of 0.14, while, in case the 2Bg configuration is considered, the pressing force on each block and the corresponding friction coefficient are equal to 5.24 kN and 0.18, respectively. Figure 6 shows for both cases the friction heat flux flowing into the wheel at the wheel-shoe interface. Obviously, the heat flux is higher for the 1Bg configuration, as only one contact interface, which must provide the required braking torque, is present.

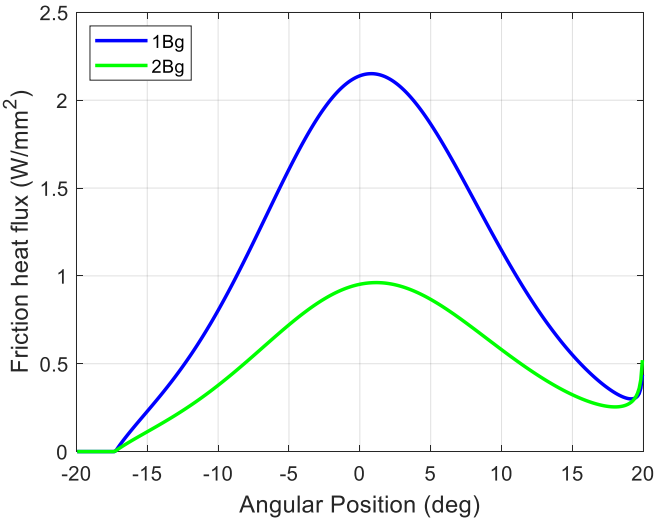

Figure 6. Heat flux distribution for 2Bg and 1Bg block configurations for the same braking operation.

Figure 7 shows the temperature evolution on a node located on the wheel surface during the drag braking operation, computed with the thermal module. As expected, the temperature for the 1Bg configuration is

higher, due to the larger heat flux flowing into the wheel at the wheel-shoe contact interface. The zoomed view at the bottom in figure 7 shows that the temperature rise due to the contact with the shoe is much larger for the 1Bg configuration with respect to the 2Bg configuration. Furthermore, the difference between the maximum and minimum temperature values recorded during a single wheel revolution is far larger for the 1Bg configuration, and this means that the 1Bg configuration can be more harmful from a thermal point of view. Finally, the detailed view in the upper left corner of figure 7 highlights a steeper temperature drop when the node is not in contact with the rail due to the rail chill effect.

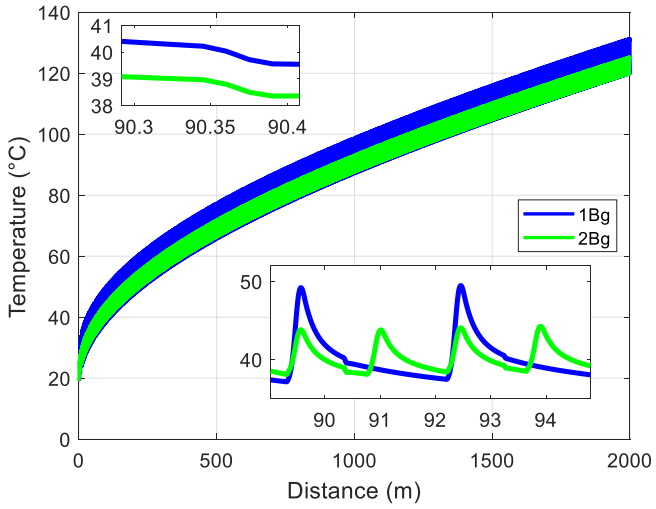

Figure 7. Wheel surface temperature during a 2 km drag braking operation at 60 km/h for 1Bg and 2Bg arrangements.

Lastly, figure 8 shows the temperature at the end of the simulation for different radial positions, and it can be noticed that the wheel is heating only in a limited range of radial coordinates where a steep temperature gradient can be observed, while the central part of the wheel is still at the initial temperature of 20°C. Therefore, since the temperature stresses and strains concern a limited peripheral portion of the wheel, it can be concluded that, as expected, local defects can arise in a limited radial sector of the wheel, and a thermal model is essential to predict the maximum wheel temperature during a braking operation, as it is not an easy task to provide the vehicle with on-board temperature sensors able to perform measurements on the external surface.

A big concern of the proposed model is the computational time, with the bottleneck of the computation obviously being the numerical integration of the o.d.es solved in the thermal module. In fact, the simulations described above, run on a computer featuring a Windows 10 Pro OS, 64-GB internal memory and an Intel 8-core i9 processor, took 2h 18 min for the 1Bg configuration and 2h 30 min for the 2Bg arrangement, thus being 69 and 75 times slower than real time, respectively. Therefore, in the author's opinion, the introduction of simplifying hypotheses, such as the development of a 2D model of a limited portion of the wheel, supported by experimental data for the model calibration, are crucial for the code to provide accurate outputs in a reasonable amount of time.

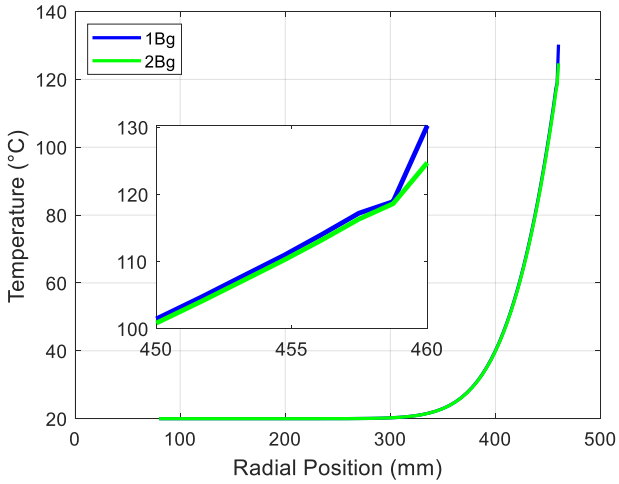

Figure 8. Temperature at the end of the drag braking simulation for different radial positions.

5. Conclusions

The paper shows the development, implementation and preliminary validation of a tool for the estimation of the temperature field produced in tread braked wheels during drag braking operations. The tool includes an external Matlab routine, for the calculation of the wheel-shoe contact force, and two FE modules implemented in ANSYS Mechanical APDL, namely a static structural contact module and a transient thermal module. The contact algorithm implemented in the structural module considers both friction and sliding at the contact interface, which lead to an asymmetry in the pressure distribution and in a peak at the leading edge, which is related to a block jamming effect. The thermal module calculates the temperature evolution due to friction heat flux, air convection and rail chill. The wheel is considered as fixed and rotating thermal loads are applied to its surface, thanks to the definition of proper ANSYS tables, which are a powerful data type for the application of time and space varying loads.

The computational effort is a primary concern in the context of this activity, and to keep the computational times as short as possible, the two FE models are decoupled, i.e., the interaction between the contact pressure and the surface temperature, as well as wear phenomena, are neglected. Furthermore, only a 45° sector of the wheel is modelled in the thermal module, with the definition of an adiabatic boundary condition at the lateral edges, under the assumption that the heat conduction in circumferential direction has a minor impact with respect to the heat transfer in radial direction. However, a good match was observed between the outputs of the reduced model and a model of the full wheel, thus confirming the validity of such hypothesis.

The preliminary simulations presented in the paper showed that the code provides results in good agreement with the expectations, and also proved that the 1Bg configuration can be more dangerous in terms of thermal stresses and strains in the wheel with respect to 2Bg configuration, under the same braking operation.

Much work is still needed to obtain a full validation of the code, which however needs to be performed against a large set of experimental data. Therefore, the author's research team is currently verifying the feasibility of designing a scaled rig for the reproduction of different braking maneuvers with all kinds of shoe material, in order to calibrate the tool parameters, keeping the computational times short. Furthermore, the code could undergo several upgrades, such as the coupling of the structural and thermal modules and the introduction of a wear module, however always paying great attention to computing speeds.

References

[1] Günay M, Korkmaz M E and Özmen R 2020 An investigation on braking systems used in railway vehicles *Eng. Sci. Technol. an Int. J.* **23** 421-31
[2] Fec M C and Sehitoglu H 1985 Thermal-mechanical damage in railroad wheels due to hot spotting *Wear* **102** 31-42
[3] Vernersson T and Lundén R 2007 Temperatures at railway tread braking. Part 3: Wheel and block

temperatures and the influence of rail chill *Proc. Inst. Mech. Eng. F: J. Rail Rapid Transit* **221** 443-54
[4] Vakkalagadda M R K, Vineesh K P and Racherla V 2015 Estimation of railway wheel running temperatures using a hybrid approach *Wear* **328-329** 537-51
[5] Cantone L and Ottati A 2018 Modelling of friction coefficient for shoes type LL by means of polynomial fitting *Open Transp. J.* **12** 114-27
[6] Vakkalagadda M R K, Srivastava D K, Mishra A and Racherla V 2015 Performance analyses of brake blocks used by indian railways *Wear* **328-329** 64-76
[7] Bosso N, Magelli M and Zampieri N 2020 Calibration and development of a multi-axis roller bench for monitoring the braking system of a railway vehicle *Ing. Ferrov.* **75** 501-23
[8] Bosso N, Magelli M and Zampieri N 2020 Validation of a brake monitoring system using a multi-axle roller-rig *WIT Transactions on The Built Environment* vol 199, ed G Passerini, J M Mera and R Takagi (Southampton, UK: WIT Press) pp. 151-62
[9] Somà A, Aimar M and Zampieri N 2021 Simulation of the thermal behavior of cast iron brake block during braking maneuvers *Appl. Sci.* **11** 5010
[10] Ertz M and Knothe K 2002 A comparison of analytical and numerical methods for the calculation of temperatures in wheel/rail contact *Wear* **253** 498-508
[11] Knothe K and Liebelt S 1995 Determination of temperatures for sliding contact with applications for wheel-rail systems *Wear* **189** 91-9
[12] Tudor A and Khonsari M M 2006 Analysis of heat partitioning in wheel/rail and wheel/brake shoe friction contact: An analytical approach *Tribol. Trans.* **49** 635-42
[13] Tudor A, Radulescu C and Petre I 2003 Thermal effect of the brake shoes friction on the wheel/rail contact *Tribol. Ind.* **25** 27-32
[14] Haidari A and Hosseini-Tehrani P 2014 Fatigue analysis of railway wheels under combined thermal and mechanical loads *J. Therm. Stresses* **37** 34-50
[15] Haidari A and Tehrani P H 2015 Thermal load effects on fatigue life of a cracked railway wheel *Lat. Am. J. Solids Struct.* **12** 1144-57
[16] Milošević M, Stamenković D, Tomić M, Milojević A and Mijajlović M 2012 Modeling thermal effects in braking systems of railway vehicles *Therm. Sci.* **16** S515-S26
[17] Pradhan S and Samantaray A K 2019 A recursive wheel wear and vehicle dynamic performance evolution computational model for rail vehicles with tread brakes *Vehicles* **1** 88-115
[18] Faccoli M, Ghidini A and Mazzù A 2018 Experimental and numerical investigation of the thermal effects on railway wheels for shoe-braked high-speed train applications *Metall. Mater. Trans. A* **49** 4544-54
[19] Vernersson T and Lundén R 2010 Wear of disc brakes and block brakes–influence of design on modelled wear for repeated brake cycles *Proceeding of the 16th International Wheelset Congress (IWC16)* (Cape Town)
[20] Petereson M 2002 Two-dimensional finite element simulation of the thermal problem at railway block braking *Proc. Inst. Mech. Eng. C: J. Mech. Eng. Sci.* **216** 259-73
[21] Suresh Babu A and Siva Prasad N 2009 Coupled field finite element analysis of railway block brakes *Proc. Inst. Mech. Eng. F: J. Rail Rapid Transit* **223** 345-52
[22] Teimourimanesh S, Vernersson T and Lundén R 2014 Modelling of temperatures during railway tread braking: Influence of contact conditions and rail cooling effect *Proc. Inst. Mech. Eng. F: J. Rail Rapid Transit* **228** 93-109
[23] Thuresson D 2004 Influence of material properties on sliding contact braking applications *Wear* **257** 451-60
[24] UIC 544-1:2014 *Brakes - braking performance*
[25] Bosso N, Magelli M and Zampieri N 2020 Long train dynamic simulation by means of a new in-house code *WIT Transactions on The Built Environment* vol 199, ed G Passerini, J M Mera and R Takagi (Southampton, UK: WIT Press) pp. 249-59
[26] Bosso N, Magelli M and Zampieri N 2021 Development and validation of a new code for longitudinal train dynamics simulation *Proc. Inst. Mech. Eng. F: J. Rail Rapid Transit* **235** 286-99
[27] Bosso N, Magelli M, Rossi Bartoli L and Zampieri N 2021 The influence of resistant force equations

and coupling system on long train dynamics simulations *Proc. Inst. Mech. Eng. F: J. Rail Rapid Transit*

[28] Spiryagin M, Wu Q and Cole C 2017 International benchmarking of longitudinal train dynamics simulators: Benchmarking questions *Veh. Syst. Dyn.* **55** 450-63

[29] Wu Q*, et al.* 2018 International benchmarking of longitudinal train dynamics simulators: Results *Veh. Syst. Dyn.* **56** 343-65

[30] Ryaben'kii V S and Tsynkov S V 2006 Numerical solution of nonlinear equations and systems *A theoretical introduction to numerical analysis* (Boca Raton, FL, USA: Chapman and Hall/CRC)

[31] Cantone L 2011 Traindy: The new union internationale des chemins de fer software for freight train interoperability *Proc. Inst. Mech. Eng. F: J. Rail Rapid Transit* **225** 57-70

[32] Simo J C and Laursen T A 1992 An augmented Lagrangian treatment of contact problems involving friction *Comput. Struct.* **42** 97-116

[33] Vernersson T 2007 Temperatures at railway tread braking. Part 2: Calibration and numerical examples *Proc. Inst. Mech. Eng. F: J. Rail Rapid Transit* **221** 429-41

[34] Churchill S W and Bernstein M 1977 A correlating equation for forced convection from gases and liquids to a circular cylinder in crossflow *J. Heat Transfer* **99** 300-6

[35] UIC 542:2010 *Brake parts - interchangeability*

[36] Crank J and Nicolson P 1947 A practical method for numerical evaluation of solutions of partial differential equations of the heat-conduction type *Math. Proc. Cambridge* **43** 50-67

[37] EN 13979:2020 *Railway applications - wheelsets and bogies - monobloc wheels - technical approval procedure* Part 1: Forged and rolled wheels